fractal and fractional

MDPI

Article

Numerical Identification of External Boundary Conditions for Time Fractional Parabolic Equations on Disjoint Domains

Miglena N. Koleva [1,*] and Lubin G. Vulkov [2]

[1] Department of Mathematics, Faculty of Natural Sciences and Education, University of Ruse "Angel Kanchev", 7017 Ruse, Bulgaria
[2] Department of Applied Mathematics and Statistics, Faculty of Natural Sciences and Education, University of Ruse "Angel Kanchev", 7017 Ruse, Bulgaria
* Correspondence: mkoleva@uni-ruse.bg; Tel.: +359-82-888-587

Abstract: We consider fractional mathematical models of fluid-porous interfaces in channel geometry. This provokes us to deal with numerical identification of the external boundary conditions for 1D and 2D time fractional parabolic problems on disjoint domains. First, we discuss the time discretization, then we decouple the full inverse problem into two Dirichlet problems at each time level. On this base, we develop decomposition techniques to obtain exact formulas for the unknown boundary conditions at point measurements. A discrete version of the analytical approach is realized on time adaptive mesh for different fractional order of the equations in each of the disjoint domains. A variety of numerical examples are discussed.

Keywords: Caputo fractional derivative; problems on disjoint domains; inverse problems; external boundary conditions; difference scheme

Citation: Koleva, M.N.; Vulkov, L.G. Numerical Identification of External Boundary Conditions for Time Fractional Parabolic Equations on Disjoint Domains. *Fractal Fract.* **2023**, 7, 326. https://doi.org/10.3390/fractalfract7040326

Academic Editor: Rodica Luca

Received: 17 February 2023
Revised: 7 April 2023
Accepted: 11 April 2023
Published: 13 April 2023

1. Introduction

A typical inverse problem is the identification of a coefficient or right-hand side in partial differential equation, at given initial and boundary conditions with over-specified data as internal or boundary observations, see, e.g., [1–3]. Problems of this type have been studied fairly well.

Many practical problems, such as heat conduction or financial engineering, are modeled by inverse problems with unknown internal or external boundary conditions, see e.g., [4–6].

Interface problems for differential equations are generally those problems in which the input data are non-smooth or discontinuous or singular across one or more lines or surfaces in the solution domain.

In this paper, we consider a special kind of interface problem that models processes situated in disjoint domains. Many approaches were applied for the case of classical parabolic or elliptic operators, see e.g., [7–13]. However, we are mainly interested in the subdiffusion model, involving fractional derivatives. In the present study, we utilize the Caputo derivative in time, which has been widely used for describing the anomalous diffusion phenomena [14–17].

In recent years, there has been extensive research on numerical solutions to interface problems. We point out the papers [18–28] closely related to the present work. In [27] a stationary nonlinear 1D problem defined on non-connected layers is considered. Well-posedness is proved and a convergent monotone iterative method has been developed. For the same problem in [21] it is constructed a finite element discretization and conditions under which the discrete maximum principle holds are investigated. In [22] is analyzed finite element method and two-grid algorithm for 2D elliptic transmission problems on disjoint domains, coupled with interface conditions on a part of the boundary. In [24] is performed an analysis of parabolic heat mass transfer problems on partitioned domains.

The existence and uniqueness of weak solutions in appropriate Sobolev-like spaces are established and a priori estimates are obtained. Authors of [20] investigate the parabolic problem on disjoint rectangular domains and prove the existence and uniqueness of a weak solution. Also, they construct and analyze finite difference approximation for solving the problem. In [18] a second-order transmission problem across a Koch-type interface is considered. A priori error estimates are proved and numerical discretization, based on the Galerkin method and θ-method in time, is developed. Authors of [28] study a linear 2D parabolic problem on nonsmooth non-convex polygonal domains. They prove the well-posedness of the problem using suitable weighted Sobolev spaces and construct discrete finite element schemes on graded meshes.

Numerical methods for time-fractional parabolic problems on disjoint domains are developed in [29,30]. Authors discussed well-posedness and obtain a priori estimates for the weak solution. Moreover, a finite difference approximation is constructed.

A fast convergent numerical approach, based on reproducing kernel functions and shooting method, is developed in [31] for solving 1D interface problems of fractional order with Caputo derivative.

Direct problems, defined on disjoint domains, are well studied in the literature, while results for the corresponding inverse problems, especially of fractional order, and most of all, of different fractional order, in each domain, are missing. The present work contributes to filling this gap.

An inverse boundary problem for the classical heat equation is solved numerically in [32]. Simultaneous recovering of source term and initial value in integer order parabolic transmission problem is considered in [33]. The inverse problem is defined as an optimization problem and the existence and stability of the solutions are analyzed.

In [34] authors prove the uniqueness of the inverse problem for identifying time-dependent smooth coefficients from measurements at part of the boundary in a time-fractional parabolic problem. The uniqueness of the solution of inverse boundary problem and inverse problem for identifying heat source density for nonlocal problems for time fractional subdiffusion equations are studied in [35].

The inverse coefficient problem with measured data at the boundary for time fractional parabolic partial differential equation with nonlocal boundary conditions is solved numerically in [36].

In this paper we consider inverse time-fractional parabolic problems on disjoint domains, including the case of different fractional order of equations in its domains. We are interested in the numerical identification of external boundary conditions on the base of internal point observations. Let us note that for second-order ordinary differential equations on disjoint domains, the semilinear inverse problem is studied in our previous conference paper [4].

The layout of the paper is as follows. In Section 2, the formulation of direct and inverse problems is presented. In Section 3 we prove the existence and uniqueness of the solution of the direct problem. A solution to the semidiscrete inverse problem is obtained in Section 4. In Section 5 we propose the numerical solution of the direct and inverse problems and discuss the implementation algorithms. An extension of the 2D problem is proposed in Section 6. Numerical simulations for 1D and 2D test examples are discussed in Section 7. We end the paper with some conclusions.

2. Direct and Inverse Problems

In this section, we formulate the 1D direct and inverse problems. As a model example, we consider the following initial boundary value problem

$$\frac{\partial^{\delta_1} u_1}{\partial t^{\delta_1}} - \frac{\partial}{\partial x}\left(p_1(x)\frac{\partial u_1}{\partial x}\right) = f_1(x,t), \quad x \in \Omega_1 = (a_1, b_1), \quad 0 < t \le T, \tag{1}$$

$$\frac{\partial^{\delta_2} u_2}{\partial t^{\delta_2}} - \frac{\partial}{\partial x}\left(p_2(x)\frac{\partial u_2}{\partial x}\right) = f_2(x,t), \quad x \in \Omega_2 = (a_2, b_2), \quad 0 < t \le T, \tag{2}$$

with external boundary conditions

$$u_1(a_1,t) = \varphi_1(t), \quad u_2(b_2,t) = \varphi_2(t), \quad 0 < t \le T, \tag{3}$$

and interface mixed-type boundary conditions

$$p_1(b_1)\frac{\partial u_1}{\partial x}(b_1,t) + \alpha_1 u_1(b_1,t) = \beta_1 u_2(a_2,t) + \gamma_1(t), \quad 0 < t \le T, \tag{4}$$

$$-p_2(a_2)\frac{\partial u_2}{\partial x}(a_2,t) + \alpha_2 u_2(a_2,t) = \beta_2 u_1(b_1,t) + \gamma_2(t), \quad 0 < t \le T, \tag{5}$$

where $-\infty < a_1 < b_1 < a_2 < b_2 < \infty$, $p_j \in L_\infty(\Omega_j)$,

$$\beta_1\beta_2 \le \alpha_1\alpha_2, \quad p_j(x) \ge \overline{p}_j > 0, \quad x \in \Omega_j, \quad j = 1,2. \tag{6}$$

and α_j, β_j, $j = 1,2$ are given constants. The fractional time derivative is in Caputo sense [14,15,37]

$$\frac{\partial^{\delta_j} u_j}{\partial t^{\delta_j}} = \frac{1}{\Gamma(1-\delta_j)}\int_0^t (t-s)^{-\delta_j}\frac{\partial u_j}{\partial s}ds, \quad 0 < \delta_j < 1, \quad j = 1,2, \tag{7}$$

where $\Gamma(\cdot)$ is Gamma function.

The problem (1)–(5) is completed with initial conditions

$$u_1(x,0) = u_1^0(x), \quad x \in \Omega_1, \quad u_2(x,0) = u_2^0(x), \quad x \in \Omega_2. \tag{8}$$

The direct (forward) problem is to find the solution $(u_1(x,t), u_2(x,t))$ of (1)–(8) at given coefficients, initial, boundary and interface conditions.

In the *external boundary conditions inverse problem* (1)–(6), the functions $\varphi_1(t)$ and/or $\varphi_2(t)$ are *unknown* and must to be identified using some over-specified data. Depending on the observation data, the *inverse problem* (IP) for identifying the external boundary condition(s) (3) can be formulated as follows:

IP[1a]: Given observation $u_1(x_1^*,t) = \psi_1(t)$, $x_1^* \in \Omega_1$. Find $(u_1, u_2, \varphi_1(t))$;

IP[1b]: Given observation $u_2(x_2^*,t) = \psi_2(t)$, $x_2^* \in \Omega_2$. Find $(u_1, u_2, \varphi_2(t))$;

IP[2a]: Given observation $u_1(x_1^*,t) = \psi_1(t)$, $x_1^* \in \Omega_1$. Find $(u_1, u_2, \varphi_2(t))$;

IP[2b]: Given observation $u_2(x_2^*,t) = \psi_2(t)$, $x_2^* \in \Omega_2$. Find $(u_1, u_2, \varphi_1(t))$;

IP[3] : Given observations $u_j(x_j^*,t) = \psi_j(t)$, $x_j^* \in \Omega_j$, $j = 1,2$. Find $(u_1, u_2, \varphi_1(t), \varphi_2(t))$.

Existence and uniqueness of the solution of the direct problem (1)–(8) and the corresponding inverse problems IP[1a]–IP[3] are not studied in the literature. In [30] is considered the particular case of the problem (1)–(8), when $\delta_1 = \delta_2 = \delta$, $0 < \delta < 1$ and instead of Caputo's derivative the Riemann-Liouville derivative is used and in [29] additionally $p_1(x,t) = p_2(x,t) \equiv 1$ is assumed.

In the next section we generalize the results in [29,30] and establish the existence and uniqueness of the solution of the direct problem (1)–(8).

3. Existence and Uniqueness of the Solution of the Direct Problem

Direct problems are in general well-posed by the concept of [38], if they satisfy: the solution to the problem exists and it is unique, the solution depends continuously on the input data. The well-posedness of elliptic and parabolic problems on disjoint domains were studied in papers [21,22,27].

Here we extend the results in [29,30] to the problem (1)–(8).

Further, in order to simplify the exhibition, we suppose homogeneous boundary conditions, namely

$$\varphi_j(t) = 0, \quad \gamma_j(t) = 0, \quad j = 1,2, \quad 0 < t \le T \tag{9}$$

and initial conditions

$$u_j^0(x) = 0, \quad j = 1,2. \tag{10}$$

We now introduce new unknown functions

$$U_1(x,t) = U_1^1(x,t) - A_1(t)(x-a_1)(x-b_1), \quad A_1(t) = \frac{\gamma_1(t)}{p_1(b_1)(b_1-a_1)},$$
$$U_2(x,t) = U_2^1(x,t) - A_2(t)(x-a_2)(x-b_2), \quad A_2(t) = \frac{\gamma_2(t)}{p_2(a_2)(b_2-a_2)},$$

where

$$U_1^1(x,t) = u_1(x,t) - \varphi_1(t) - u_1^0(x),$$
$$U_2^1(x,t) = u_2(x,t) - \varphi_2(t) - u_2^0(x).$$

Thus, U_1 and U_2 satisfy the problem for equations (1), (2), in which the right-hand sides are obtained by substituting U_1 and U_2 in the left part of (1) and (2), with homogeneous boundary conditions (3)–(5), (9) and zero initial conditions (8), (10).

We introduce the alternative of the Caputo derivative, namely, the left and the right Riemann-Liouville fractional derivatives, respectively, which are defined for any integer n and $n-1 \le \delta < n$ by the

$$D_{0+}^{\delta} w(t) = \frac{1}{\Gamma(n-\delta)} \frac{d^n}{dt^n} \int_0^t \frac{w(\tau)}{(t-\tau)^{\delta-n+1}} d\tau,$$

$$D_{T-}^{\delta} w(t) = \frac{(-1)^n}{\Gamma(n-\delta)} \frac{d^n}{dt^n} \int_t^T \frac{w(\tau)}{(\tau-t)^{\delta-n+1}} d\tau.$$

The following relation between Caputo and Riemann-Liouville fractional derivatives is well-known [15]

$$\frac{\partial^{\delta} w}{\partial t^{\delta}}(x,t) = D_{0+}^{\delta} w(x,t) - \frac{w(x,0)(t)^{-\delta}}{\Gamma(1-\delta).}$$

Let $H^{\delta}(a,b)$, $H^0(a,b) = L^2(a,b)$, $\dot{H}^{\delta}(a,b)$ be the standard Sobolev spaces [39]. Further, we introduce the notations as in [29,30]. We define the spaces $H_{\pm}^{\delta}(a,b)$ and $\dot{H}_{\pm}^{\delta}(a,b)$ as the closure of $C^{\infty}[a,b]$ and $\dot{C}^{\infty}(a,b)$, with respect to the norm

$$\|u\|_{H_{\pm}^{\delta}(a,b)}^2 = \|u\|_{L^2(a,b)}^2 + |u|_{H_{\pm}^{\delta}}^2,$$

where

$$|u|_{H_{+}^{\delta}(a,b)} = \|D_{a+}^{\delta} u\|_{L_2(a,b)}, \quad |u|_{H_{-}^{\delta}(a,b)} = \|D_{b-}^{\delta} u\|_{L_2(a,b)}.$$

Note that for integer order derivative $\delta \in \mathbb{N}$, we have $H_{\pm}^{\delta}(a,b) = H^{\delta}(a,b)$.

Let $Q = (a,b) \times (0,T)$. We introduce anisotropic Sobolev space of the functions of two variables x and t, defined in Q [39]

$$H^{\delta,\nu}(Q) = L^2\big((0,T), H^{\delta}(a,b)\big) \cap H^{\nu}\big((0,T), L^2(a,b)\big).$$

Analogously, we set

$$H_{\pm}^{\delta,\nu}(Q) = L^2\big((0,T), H^{\delta}(a,b)\big) \cap H_{\pm}^{\nu}\big((0,T), L^2(a,b)\big).$$

Further, we define $Q_i = \Omega_i \times (0,T)$ and consider the product space

$$L^2 = L^2(Q_1) \times L^2(Q_2) = \{v = (v_1, v_2) | v_i \in L^2(Q_j),\ j = 1,2\},$$

endowed with the inner product and norm

$$(v,w)_{L^2} = \beta_2 (v_1, w_1)_{L^2(Q_1)} + \beta_1 (v_2, w_2)_{L^2(Q_1)},\ \ \|v\|_{L^2} = (v,v)_{L^2}^{1/2}.$$

Now, we consider the spaces

$$H^{\delta,\nu} = H^{\delta,\nu}(Q_1) \times H^{\delta,\nu}(Q_2) \ \text{ and } \ H_{\pm}^{\delta,\nu} = H_{\pm}^{\delta,\nu}(Q_1) \times H_{\pm}^{\delta,\nu}(Q_2).$$

In particular, we define

$$H_0^{1,\delta/2} = \big\{v = (v_1, v_2) : v_1 \in L^2(0,T) \cap \dot{H}^{\delta/2}\big((0,T), L^2(a_1,b_1)\big),$$
$$v_2 \in L^2\big((0,T), H^1(a_2,b_2)\big) \cap \dot{H}^{\delta/2}\big((0,T), L^2(a_2,b_2)\big),\ \ v_1(a_1,t) = v_2(b_2,t) = 0\big\}.$$

Here,

$$|v_j|_{H^{\delta}(0,T)} = \|D_{0+}^{\delta} v_j\|_{L^2(0,T)},\ \ |v_j|_{H^{\delta}(0,T)} = \|D_{T-}^{\delta} v_j\|_{L^2(0,T)},$$

and

$$\|v_j\|_{H_{\pm}^{\delta}(0,T)} = \Big(\|v_j\|_{L^2(0,T)} + \|v_j\|^2_{H_{\pm}^{\delta}(0,T)}\Big)^{1/2},\ \ j = 1,2.$$

In the next theorem the integration by parts formula [15] plays a key role. For all $0 < \delta < 1$, if $w \in C^2[0,T]$ and $w(0) = 0,\ v \in C_0^{\infty}[0,T]$, then

$$\begin{aligned} &\int_0^T \frac{\partial^{\delta} w}{\partial t^{\delta}}(t) v(t) dt = \int_0^T D_{0+}^{\delta/2} w(t) D_{T-}^{\delta/2} v(t) dt, \\ &\left(\frac{\partial^{\delta} w}{\partial t^{\delta}}, v\right)_{L^2(0,T)} = \left(D_{0+}^{\delta/2} w, D_{T-}^{\delta/2} v\right)_{L^2(0,T)}. \end{aligned} \tag{11}$$

The weak formulation of the problem (1)–(8) has the form $u = (u_1, u_2)$, $u_i \in H_0^{1,\delta_j/2}$, such that

$$a(u,v) = l(v),\ \ \forall v = (v_1, v_2),\ \ v_j \in H_0^{1,\delta_j/2},\ \ j = 1,2,$$

where

$$\begin{aligned} a(u,v) &= a_1(u_1, v_1) + a_2(u_2, v_2) + a_3(u,v), \\ a_j(u_j, v_j) &= \beta_{3-j}\Big(D_-^{\delta_j/2} u_i, D_+^{\delta_j/2} v_j\Big)_{L^2(Q_j)} + \beta_{3-j}\left(p_j \frac{\partial u_j}{\partial x}, \frac{\partial v_j}{\partial x}\right)_{L^2(Q_j)},\ \ j = 1,2, \\ a_3(u,v) &= \int_0^T \big[\beta_2 \alpha_1 u_1(b_1,t) v_1(b_1,t) + \beta_1 \alpha_2 (a_2,t) v_1(a_2,t) \\ &\quad - \beta_1 \beta_2 [u_1(b_1,t) v_2(a_2,t) + u_2(a_2,t) v_1(b_1,t)]\big] dt, \\ l(v) &= (f,v)_{L^2} = \beta_2 (f_1, v_1)_{L^2(Q_1)} + \beta_1 (f_2, v_2)_{L^2(Q_2)}. \end{aligned}$$

The following assertion holds.

Theorem 1. *Let the conditions* (6) *be satisfied. Then, the problem* (1)–(8) *is well-posed and the following a priori estimate holds*

$$\|u_1\|_{H^{1,\delta_1/2}} + \|u_2\|_{H^{1,\delta_2/2}} \le C\Big(\|f_1\|_{L_2(Q_1)} + \|f_2\|_{L_2(Q_2)}\Big).$$

Proof. We use formula (11) of integration by parts and ([29], Lemmas 1–3) . Then, we apply Cauchy-Schwarz and Poincaré inequalities [39] and, taking into account the inequality $\beta_1\beta_2 \le \alpha_1\alpha_2$ in (6), we prove that the bilinear form $a(u,v)$, together with linear functional $l(\cdot)$ satisfy the requirements of the Lax-Milgram lemma [39]. □

4. Solution of the Semidiscrete Direct and Inverse Problem

In this section, we develop a decomposition technique for solving inverse problems IP[1a]–IP[3]. The more efficient way to realize this approach is to decouple the discrete system at each time level. In this case, we have to solve four small discrete systems-two in each discretized interval $\overline{\Omega}_1 = [a_1, b_1]$ and $\overline{\Omega}_2 = [a_2, b_2]$. Otherwise, without a decoupling procedure, at each time level, we have to solve three large systems on the discretized interval $\overline{\Omega}_1 \cup \overline{\Omega}_2$.

The problem of decoupling the discrete system can be tackled in different ways. For example, using the left and right Thomas method for the numerical solution of the discrete equations [4,22], or utilizing measurement data [4]. In this work, the decoupling is based on implicit-explicit time stepping.

4.1. Time Semidiscretization of the Direct Problem

The starting point for our decomposition method is the temporal semi-discretization of the direct problem (1)–(8).

Let us define the nonuniform temporal mesh $\overline{\omega}_\tau$: $0 = t_0 < t_1 < \cdots < t_M = T$ with step size $\tau_{n+1} = t_{n+1} - t_n$, $n = 0, 1, \ldots, M-1$, $\tau_n < \tau_{n+1}$ and $\tau = \max\limits_{0\le n\le M} \tau_n$. Denote by $u_j^n = u_j^n(x) = u_j(t_n, x)$, $j = 1, 2$. The Caputo fractional derivative of the function u_j^{n+1} is approximated by $L1$ formula on non-uniform mesh [16,17]

$$\begin{aligned}\frac{\partial^{\delta_j} u_j^{n+1}(x)}{\partial t^{\delta_j}} &\approx \frac{1}{\Gamma(1-\delta_j)} \sum_{s=0}^{n} \frac{u_j^{s+1}(x) - u_j^s(x)}{\tau_{s+1}} \int\limits_{t_s}^{t_{s+1}} (t_{n+1} - \eta)^{-\delta_j} d\eta \\ &= \sum_{s=0}^{n} (u_j^{s+1} - u_j^s)\rho_{n,s}^j,\end{aligned}$$

where

$$\rho_{n,s}^j = \frac{(t_{n+1} - t_s)^{1-\delta_j} - (t_{n+1} - t_{s+1})^{1-\delta_j}}{\Gamma(2-\delta_j)\tau_{s+1}} \quad \text{and} \quad \rho_{n,n}^j = \frac{\tau_{n+1}^{-\delta_j}}{\Gamma(2-\delta_j)}.$$

We consider the following semi-implicit time discretization of the problem (1)–(8)

$$\rho^1_{n,n}u_1^{n+1} - \frac{\partial}{\partial x}\left(p_1(x)\frac{\partial u_1^{n+1}}{\partial x}\right) = f_1^{n+1}(x) + G_n^1 u_1^n(x), \quad x \in \Omega_1 = (a_1, b_1), \tag{12}$$

$$\rho^2_{n,n}u_2^{n+1} - \frac{\partial}{\partial x}\left(p_2(x)\frac{\partial u_2^{n+1}}{\partial x}\right) = f_2^{n+1}(x) + G_n^2 u_2^n(x), \quad x \in \Omega_2 = (a_2, b_2), \tag{13}$$

$$u_1^{n+1}(a_1) = \varphi_1^{n+1}, \quad u_2^{n+1}(b_2) = \varphi_2^{n+1}, \tag{14}$$

$$p_1(b_1)\frac{\partial u_1^{n+1}}{\partial x}(b_1) + \alpha_1 u_1^{n+1}(b_1) = \beta_1 u_2^n(a_2) + \gamma_1^{n+1}, \tag{15}$$

$$-p_2(a_2)\frac{\partial u_2^{n+1}}{\partial x}(a_2) + \alpha_2 u_2^{n+1}(a_2) = \beta_2 u_1^n(b_1) + \gamma_2^{n+1}, \tag{16}$$

together with initial conditions (8). Here

$$G_n^j u_j^n(x) := \sum_{s=1}^{n}\left(\rho^j_{n,s} - \rho^j_{n,s-1}\right)u_j^s(x) + \rho^j_{n,0}u_j^0(x), \quad n = 0, 1, \ldots, M-1.$$

The direct semidiscrete problem is defined by (8) and (12)–(16), where the unknown solution is $u_j^{n+1}(x)$, $j = 1, 2$, $n = 0, 1, \ldots, M-1$ and all input data—coefficient functions, right-hand sides, initial and boundary conditions—are known.

Note that at each time level $n = 0, 1, \ldots, M$, we solve the problems (12), (14), (15), (8) (first equations) in $\overline{\Omega}_1$ and (13), (14), (16), (8) (second equations) in $\overline{\Omega}_2$ separately.

4.2. Solving the Inverse Problems

The semidiscrete inverse problem is to find the solution $u_j^{n+1}(x)$, $j = 1, 2$, φ_1^{n+1} and/or φ_2^{n+1} (in convention with IP[1a]–IP[3]), $n = 0, 1, \ldots, M-1$, solving the problem (8)–(12), where left or/and right external boundary conditions (14) are not known and we have additional observations $u_1^{n+1}(x^*) = \psi_1^{n+1}(x^*)$ or/and $u_2^{n+1}(x^*) = \psi_2^{n+1}(x^*)$, depending on the inverse problem IP[1a]-IP[3].

To find approximate solution (u_1^{n+1}, u_2^{n+1}), we consider the following solution decomposition

$$u_1^{n+1} = v_1^{n+1} + \widetilde{\varphi}_1^{n+1}w_1^{n+1}, \tag{17}$$

$$u_2^{n+1} = v_2^{n+1} + \widetilde{\varphi}_2^{n+1}w_2^{n+1}, \tag{18}$$

where $\widetilde{\varphi}_j^{n+1}$, $j = 1, 2$ are unknown and

$$\begin{array}{ll}
\widetilde{\varphi}_1^{n+1} = \varphi_1^{n+1}, \ v_2^{n+1} = u_2^{n+1}, \ \widetilde{\varphi}_2^{n+1} = 0 & \text{for IP[1a]},\\
\widetilde{\varphi}_2^{n+1} = \varphi_2^{n+1}, \ v_1^{n+1} = u_1^{n+1}, \ \widetilde{\varphi}_1^{n+1} = 0 & \text{for IP[1b]},\\
\widetilde{\varphi}_1^{n+1} = \widetilde{\varphi}_2^{n+1} = \varphi_2^{n+1}, & \text{for IP[2a]},\\
\widetilde{\varphi}_1^{n+1} = \widetilde{\varphi}_2^{n+1} = \varphi_1^{n+1}, & \text{for IP[2b]},\\
\widetilde{\varphi}_1^{n+1} = \varphi_1^{n+1}, \ \widetilde{\varphi}_2^{n+1} = \varphi_2^{n+1}, & \text{for IP[3]}.
\end{array}$$

Let us turn to the IP[3]. Substituting (17) and (18) in (12)–(16) and in view of (8), we get four independent (at each time level) direct problems

$$\begin{aligned}
&\rho^1_{n,n}v_1^{n+1} - \frac{\partial}{\partial x}\left(p_1(x)\frac{\partial v_1^{n+1}}{\partial x}\right) = f_1^{n+1}(x) + G_n^1 u_1^n(x), \quad x \in \Omega_1,\\
&v_1^{n+1}(a_1) = 0,\\
&p_1(b_1)\frac{\partial v_1^{n+1}}{\partial x}(b_1) + \alpha_1 v_1^{n+1}(b_1) = \beta_1 u_2^n(a_2) + \gamma_1^{n+1},\\
&u_1^0 = u_1^0(x).
\end{aligned} \tag{19}$$

$$\begin{aligned}
&\rho^2_{n,n} v_2^{n+1} - \frac{\partial}{\partial x}\left(p_2(x)\frac{\partial v_2^{n+1}}{\partial x}\right) = f_2^{n+1}(x) + G_n^2 u_2^n(x), \;\; x \in \Omega_2,\\
&-p_2(a_2)\frac{\partial v_2^{n+1}}{\partial x}(a_2) + \alpha_2 v_2^{n+1}(a_2) = \beta_2 u_1^n(b_1) + \gamma_2^{n+1},\\
&v_2^{n+1}(b_2) = 0,\\
&u_2^0 = u_2^0(x).
\end{aligned} \tag{20}$$

$$\begin{aligned}
&\rho^1_{n,n} w_1^{n+1} - \frac{\partial}{\partial x}\left(p_1(x)\frac{\partial w_1^{n+1}}{\partial x}\right) = 0, \;\; x \in \Omega_1,\\
&w_1^{n+1}(a_1) = 1,\\
&p_1(b_1)\frac{\partial w_1^{n+1}}{\partial x}(b_1) + \alpha_1 w_1^{n+1}(b_1) = 0.
\end{aligned} \tag{21}$$

$$\begin{aligned}
&\rho^2_{n,n} w_2^{n+1} - \frac{\partial}{\partial x}\left(p_2(x)\frac{\partial w_2^{n+1}}{\partial x}\right) = 0, \;\; x \in \Omega_2,\\
&-p_2(a_2)\frac{\partial w_2^{n+1}}{\partial x}(a_2) + \alpha_2 w_2^{n+1}(a_2) = 0,\\
&w_2^{n+1}(b_2) = 1.
\end{aligned} \tag{22}$$

Further, from additional data given for IP[3], namely the observations $u_j^{n+1}(x_j^*) = \psi_j^{n+1}$, $x_j^* \in \Omega_j$, $j = 1, 2$, we derive

$$\varphi_j^{n+1} = \frac{\psi_j^{n+1} - v_j^{n+1}(x_j^*)}{w_j^{n+1}(x_j^*)}, \;\; j = 1, 2. \tag{23}$$

For solving IP[1a] and IP[1b] we apply the decomposition only in one of the domains-Ω_1 or Ω_2, where is the point of measurement. Namely, to recover φ_1 in IP[1a], at each time level we solve (13), (14) (second equation), (16), starting with the corresponding initial condition (8), and (19), (21). Then, we use (23), $j = 1$ to find the left external boundary condition.

In the same manner, we deal with IP[1b]. At each time level we solve consequently direct problems: (12), (14) (first equation), (15) with the corresponding initial condition (8), and (20), (22). To restore the right external boundary condition, we utilize (23), $j = 2$.

Regarding IP[2a] and IP[2b], we proceed as follows. To identify φ_1 (IP[2a]), we solve (20), (22) and then problems similar to (19), (21), but with modified boundary conditions, namely

$$\begin{aligned}
&\rho^1_{n,n} v_1^{n+1} - \frac{\partial}{\partial x}\left(p_1(x)\frac{\partial v_1^{n+1}}{\partial x}\right) = f_1^{n+1}(x) + G_n^1 u_1^n(x), \;\; x \in \Omega_1,\\
&v_1^{n+1}(a_1) = \varphi_1^{n+1},\\
&p_1(b_1)\frac{\partial v_1^{n+1}}{\partial x}(b_1) + \alpha_1 v_1^{n+1}(b_1) = \beta_1 v_2^{n+1}(a_2) + \gamma_1^{n+1},\\
&u_1^0 = u_1^0(x).
\end{aligned} \tag{24}$$

$$\begin{aligned}
&\rho^1_{n,n} w_1^{n+1} - \frac{\partial}{\partial x}\left(p_1(x)\frac{\partial w_1^{n+1}}{\partial x}\right) = 0, \;\; x \in \Omega_1,\\
&w_1^{n+1}(a_1) = 0,\\
&p_1(b_1)\frac{\partial w_1^{n+1}}{\partial x}(b_1) + \alpha_1 w_1^{n+1}(b_1) = \beta_1 w_2^{n+1}(a_2).
\end{aligned} \tag{25}$$

The boundary condition at $x = b_1$ in (24) and (25) is obtained, representing $u_2^n(a_2)$ by (18). Then, we find φ_2 from (23), $j = 1$. Quantities $v_2^{n+1}(a_2)$ are $w_2^{n+1}(a_2)$ are known, since we first solve the problems (20), (22).

The decomposition method for IP[2b] is obtained similarly. To recover φ_2, we first solve (19), (22) and then problems similar to (20), (22), but with modified boundary conditions, utilizing the decomposition (17) also at old time layer. Finally, we determine φ_1 from (23), $j = 2$.

Further, we are concentrated on solving IP[3].

The crucial moment at the application of the proposed decomposition method is the validation of formula (23). A sufficient condition is given by the following assertion.

Proposition 1 (Correctness)**.** *Let in addition to the requirements* (6)*, we have* $\alpha_j \geq 0$*,* $j = 1, 2$*. Then,*

$$w_j^n(x_j^*) \neq 0, \quad j = 1, 2, \quad n = 1, \ldots, M.$$

Proof. Maximum principle for (21), (22), left boundary condition of (21) and right boundary condition of (22), implies $w_j^{n+1}(x_j) > 0$, $x_j \in \Omega_j$, $j = 1, 2$, $n = 0, 1, \ldots, M$. □

Proposition 1 guarantees the existence of the semi-discrete solution of IP[3]. With the next statement we establish uniqueness.

Theorem 2. *Let the conditions of Proposition 1 be fulfilled. Then the solution of the inverse problem* (17)–(23) *is unique.*

Proof. Suppose that the problem (17)–(23) has two solutions $(\varphi_j^1)^{n+1}$, $(\varphi_j^2)^{n+1}$ and $(u_j^1)^{n+1}$, $(u_j^2)^{n+1}$, $j = 1, 2$, $n = 0, 1, \ldots, M-1$, obtained for one and the same measured data ψ_j^{n+1}. Then, from (23) follows that at least one of the problems (19)–(22) has two solutions, denoted by $(v_j^1)^{n+1}$, $(v_j^2)^{n+1}$, $(w_j^1)^{n+1}$, $(w_j^2)^{n+1}$, $j = 1, 2$, respectively. So, we have to prove that for one and the same initial data, problem (19)–(22) has a unique solution.

Let $z_j^{n+1} = (v_j^1)^{n+1} - (v_j^2)^{n+1}$, $y_j^{n+1} = (w_j^1)^{n+1} - (w_j^2)^{n+1}$, $\bar{z}_j^{n+1} = (u_j^1)^{n+1} - (u_j^2)^{n+1}$, $j = 1, 2$. Substitute each of the solutions in the corresponding problems and subtract the equivalent problems, we get

$$\begin{aligned} &\rho_{n,n}^1 z_1^{n+1} - \frac{\partial}{\partial x}\left(p_1(x)\frac{\partial z_1^{n+1}}{\partial x}\right) = G_n^1 \bar{z}_1^n(x), \quad x \in \Omega_1, \\ &p_1(b_1)\frac{\partial z_1^{n+1}}{\partial x}(b_1) + \alpha_1 z_1^{n+1}(b_1) = \beta_1 \bar{z}_2^n(a_2), \quad z_1^{n+1}(a_1) = 0, \quad \bar{z}_1^0 = 0. \end{aligned} \tag{26}$$

$$\begin{aligned} &\rho_{n,n}^2 z_2^{n+1} - \frac{\partial}{\partial x}\left(p_2(x)\frac{\partial z_2^{n+1}}{\partial x}\right) = G_n^2 \bar{z}_2^n(x), \quad x \in \Omega_2, \\ &-p_2(a_2)\frac{\partial z_2^{n+1}}{\partial x}(a_2) + \alpha_2 z_2^{n+1}(a_2) = \beta_2 \bar{z}_1^n(b_1), \quad z_2^{n+1}(b_2) = 0, \quad \bar{z}_2^0 = 0. \end{aligned} \tag{27}$$

$$\begin{aligned} &\rho_{n,n}^1 y_1^{n+1} - \frac{\partial}{\partial x}\left(p_1(x)\frac{\partial y_1^{n+1}}{\partial x}\right) = 0, \quad x \in \Omega_1, \\ &y_1^{n+1}(a_1) = 0, \quad p_1(b_1)\frac{\partial y_1^{n+1}}{\partial x}(b_1) + \alpha_1 y_1^{n+1}(b_1) = 0. \end{aligned} \tag{28}$$

$$\begin{aligned} &\rho_{n,n}^2 y_2^{n+1} - \frac{\partial}{\partial x}\left(p_2(x)\frac{\partial y_2^{n+1}}{\partial x}\right) = 0, \quad x \in \Omega_2, \\ &- p_2(a_2)\frac{\partial y_2^{n+1}}{\partial x}(a_2) + \alpha_2 y_2^{n+1}(a_2) = 0, \quad y_2^{n+1}(b_2) = 0. \end{aligned} \tag{29}$$

Note that, at each time level, we have boundary value problems for second-order ordinary differential equations. In (28), (29) the corresponding equations and boundary conditions are homogeneous. Taking into account that $\rho_{n,n}^j > 0$, $\alpha_j \geq 0$, $j = 1,2$, and in view of (6), we conclude that $y_1^{n+1} = y_2^{n+1} = 0$, $n = 0,1,\ldots,M-1$.

Consider the problems (26), (27). Let $n = 1$. Since $\overline{z}_j^0 = 0$, we have $G_n^j \overline{z}_j^1(x) = 0$ and $\overline{z}_2^0(a_2) = \overline{z}_1^0(b_1) = 0$, $j = 1,2$. Thus we obtain homogeneous differential equations with homogeneous boundary conditions. Therefore, $z_1^1 = z_2^1 = 0$. In the same manner we get $z_1^2 = z_2^2 = 0$, since $G_n^j \overline{z}_j^1(x) = 0$ and $\overline{z}_2^1(a_2) = \overline{z}_1^1(b_1) = 0$, $j = 1,2$. We apply the same considerations advancing layer by layer in time to deduce that $z_1^{n+1} = z_2^{n+1} = 0$, $n = 0,1,\ldots,M-1$. □

5. Numerical Realization

In this section, we construct a fully discrete numerical scheme for solving inverse problem IP[3] and an algorithm for computational realization.

5.1. Full Discretizations

Since at every time layer, each of the problems (19), (20) will be solved numerically in its domain, and the problems (21), (22) are fully decoupled and independent, we introduce two uniform spatial meshes in $\overline{\Omega}_j$, $j = 1,2$

$$\overline{\omega}_j = \{x_{j,i_j} : x_{j,i_j} = a_j + i_j h_j, i_j = 0,1,\ldots,N_j, \;\; h_j = (b_j - a_j)/N_j\}, \;\; j = 1,2.$$

The function $y_j(x,t)$ at grid node (x_{j,i_j}, t_n) is denoted by y_{j,i_j}^n.

For the spatial approximation of (19)–(22), we apply the finite volume method. To this aim, we consider dual meshes of cell-centered grid nodes $x_{j,i_j-1/2} = x_{j,i_j} - \frac{h_j}{2}$, $i_j = 0,1,\ldots,N_j+1$, where $x_{j,-1/2} = x_{j,0}$, $x_{j,N_j+1/2} = x_{j,N_j}$, $j = 1,2$.

Consider the problem (19). Integrating the first equation over the volumes $(x_{1,i_1-1/2}, x_{1,i_1+1/2})$, $i_1 = 1,2,\ldots,N_1-1$, we obtain the discretization at inner grid nodes. Then we integrate the first equation in (19) over the volume $(x_{1,N_1-1/2}, x_{1,N_1})$ and using the boundary condition at $x = b_1$ we get the approximation at right boundary. In the same fashion we deal with problems (20)–(22). The resulting full discrete problems are

$$\begin{aligned} &\rho_{n,n}^1 v_{1,i_1}^{n+1} - \frac{1}{h_1}\left(p_{1,i_1+1/2} v_{1,x_{i_1}}^{n+1} - p_{1,i_1-1/2} v_{1,\overline{x}_{i_1}}^{n+1}\right) = f_{1,i_1}^{n+1} + G_n^1 u_{1,i_1}^n, \;\; i_1 = 1,2,\ldots,N_1-1, \\ &v_{1,0}^{n+1} = 0, \\ &\left(\rho_{n,n}^1 + \frac{2\alpha_1}{h_1}\right) v_{1,N_1}^{n+1} + \frac{2}{h_1} p_{1,N_1-1/2} v_{1,\overline{x}_{N_1}}^{n+1} = \frac{2\beta_1}{h_1} u_{2,0}^n + \frac{2}{h_1}\gamma_1^{n+1} + f_{1,N_1}^{n+1} + G_n^1 u_{1,N_1}^n, \\ &u_{1,i_1}^0 = u_1^0(x_{1,i_1}). \end{aligned} \tag{30}$$

$$\begin{aligned} &\rho_{n,n}^2 v_{2,i_2}^{n+1} - \frac{1}{h_2}\left(p_{2,i_2+1/2} v_{2,x_{i_2}}^{n+1} - p_{2,i_2-1/2} v_{2,\overline{x}_{i_2}}^{n+1}\right) = f_{2,i_2}^{n+1} + G_n^2 u_{2,i_2}^n, \;\; i_2 = 1,2,\ldots,N_2-1, \\ &\left(\rho_{n,n}^2 + \frac{2\alpha_2}{h_2}\right) v_{2,0}^{n+1} - \frac{2}{h_2} p_{2,1/2} v_{2,x_0}^{n+1} = \frac{2\beta_2}{h_2} u_{1,N_1}^n + \frac{2}{h_2}\gamma_2^{n+1} + f_{2,0}^{n+1} + G_n^2 u_{2,0}^n \\ &v_{2,N_2}^{n+1} = 0, \\ &u_{2,i_2}^0 = u_2^0(x_{2,i_2}). \end{aligned} \tag{31}$$

$$\begin{aligned}
&\rho^1_{n,n} w^{n+1}_{1,i_1} - \frac{1}{h_1}\left(p_{1,i_1+1/2} w^{n+1}_{1,x_{i_1}} - p_{1,i_1-1/2} w^{n+1}_{1,\bar{x}_{i_1}}\right) = 0, \;\; i_1 = 1,2,\ldots,N_1-1,\\
&w^{n+1}_{1,0} = 1,\\
&\left(\rho^1_{n,n} + \frac{2\alpha_1}{h_1}\right) w^{n+1}_{1,N_1} + \frac{2}{h_1} p_{1,N_1-1/2} w^{n+1}_{1,\bar{x}_{N_1}} = 0,
\end{aligned} \tag{32}$$

$$\begin{aligned}
&\rho^2_{n,n} w^{n+1}_{2,i_2} - \frac{1}{h_2}\left(p_{1,i_2+1/2} w^{n+1}_{2,x_{i_2}} - p_{2,i_2-1/2} w^{n+1}_{2,\bar{x}_{i_2}}\right) = 0, \;\; i_2 = 1,2,\ldots,N_2-1,\\
&\left(\rho^2_{n,n} + \frac{2\alpha_2}{h_2}\right) w^{n+1}_{2,0} - \frac{2}{h_2} p_{1,1/2} w^{n+1}_{2,x_0} = 0,\\
&w^{n+1}_{2,N_2} = 1.
\end{aligned} \tag{33}$$

Here, we use the notations

$$v_{j,x_{i_j}} = \frac{v^{n+1}_{j,i_j+1} - v^{n+1}_{j,i_j}}{h_j}, \;\; v_{j,\bar{x}_{i_j}} = \frac{v^{n+1}_{j,i_j} - v^{n+1}_{j,i_j-1}}{h_j}, \;\; p_{j,i_j\pm1/2} = p_j(x_{j,i_j\pm1/2}).$$

Further, we use the numerical solution of the direct problem (1)–(5) to verify the accuracy of the corresponding solution of the inverse problem and as perturbed data at points of the measurement. The full discretization of (1)–(5), obtained by finite volume method is

$$\begin{aligned}
&u^{n+1}_{1,0} = \varphi^{n+1}_1,\\
&\rho^1_{n,n} u^{n+1}_{1,i_1} - \frac{1}{h_1}\left(p_{1,i_1+1/2} u^{n+1}_{1,x_{i_1}} - p_{1,i_1-1/2} u^{n+1}_{1,\bar{x}_{i_1}}\right) = f^{n+1}_{1,i_1} + G^1_n u^n_{1,i_1}, \;\; i_1 = 1,2,\ldots,N_1-1,\\
&\left(\rho^1_{n,n} + \frac{2\alpha_1}{h_1}\right) u^{n+1}_{1,N_1} + \frac{2}{h_1} p_{1,N_1-1/2} u^{n+1}_{1,\bar{x}_{N_1}} = \frac{2\beta_1}{h_1} u^n_{2,0} + \frac{2}{h_1}\gamma^{n+1}_1 + f^{n+1}_{1,N_1} + G^1_n u^n_{1,N_1},\\
&\left(\rho^2_{n,n} + \frac{2\alpha_2}{h_2}\right) u^{n+1}_{2,0} - \frac{2}{h_2} p_{2,1/2} u^{n+1}_{2,x_0} = \frac{2\beta_2}{h_2} u^n_{1,N_1} + \frac{2}{h_2}\gamma^{n+1}_2 + f^{n+1}_{2,0} + G^2_n u^n_{2,0},\\
&\rho^2_{n,n} u^{n+1}_{2,i_2} - \frac{1}{h_2}\left(p_{2,i_2+1/2} u^{n+1}_{2,x_{i_2}} - p_{2,i_2-1/2} u^{n+1}_{2,\bar{x}_{i_2}}\right) = f^{n+1}_{2,i_2} + G^2_n u^n_{2,i_2}, \;\; i_2 = 1,2,\ldots,N_2-1,\\
&u^{n+1}_{2,N_2} = \varphi^{n+1}_2,\\
&u^0_{1,i_1} = u^0_1(x_{1,i_1}), \;\; u^0_{2,i_2} = u^0_2(x_{2,i_2}).
\end{aligned} \tag{34}$$

5.2. Correctness

We need to prove that $w^n_{j,i_j} \neq 0$, $i_j = 0,1,\ldots,N_j$, $j = 1,2$, $n = 1,2,\ldots,M$ in order to apply (23) at points of measurement.

Theorem 3. *Let the condition (6) be fulfilled. If $\alpha_j \geq 0$, $j = 1,2$, the solution of (32) and (33) is bounded and $0 < w^n_j \leq 1$, $j = 1,2$, $n = 1,2,\ldots,M$.*

Proof. Consider the problem (32) and rewrite it in the form, $i_1 = 1,2,\ldots,N_1-1$,

$$\begin{aligned}
&-\frac{p_{1,i_1-1/2}}{h_1} w^{n+1}_{1,i_1-1} + \left(\rho^1_{n,n} + \frac{p_{1,i_1+1/2} + p_{1,i_1-1/2}}{h_1}\right) w^{n+1}_{1,i_1} - \frac{p_{1,i_1+1/2}}{h_1} w^{n+1}_{1,i_1+1} = 0,\\
&w^{n+1}_{1,0} = 1,\\
&\left(\rho^1_{n,n} + \frac{2\alpha_1}{h_1} + \frac{2p_{1,N_1-1/2}}{h_1}\right) w^{n+1}_{1,N_1} - \frac{2}{h_1} p_{1,N_1-1/2} w^{n+1}_{1,N_1-1} = 0.
\end{aligned} \tag{35}$$

Obviously, the coefficient matrix is strictly diagonally dominant with positive main diagonal elements and nonpositive off-diagonal entries and therefore its inverse is non-negative [40]. Consequently, since the right-hand side is non-negative, we conclude that $w_{1,i_1}^{n+1} \geq 0$ for $i_1 = 0, 1, \ldots, N_1$, $n = 0, 1, \ldots, M$. Moreover, we have the following estimate

$$\|w_1^{n+1}\| \leq 1, \text{ where } \|w_1\| = \max_{0 \leq i_1 \leq N_1} |w_{1,i_1}|.$$

From the first equation in (35) for $i_1 = 1$, we get

$$\left(\rho_{n,n}^1 + \frac{p_{1,3/2} + p_{1,1/2}}{h_1}\right) w_{1,1}^{n+1} = \frac{p_{1,1/2}}{h_1} + \frac{p_{1,3/2}}{h_1} w_{1,2}^{n+1}$$

and

$$w_{1,1}^{n+1} \geq \frac{p_{1,1/2}}{h_1 \rho_{n,n}^1 + p_{1,1/2} + p_{1,3/2}} > 0.$$

Similarly, for $i_1 = 2$, we derive

$$w_{1,2}^{n+1} \geq \frac{p_{1,3/2}}{h_1 \rho_{n,n}^1 + p_{1,3/2} + p_{1,5/2}} w_{1,1}^{n+1} > 0.$$

In the same fashion, for $i_1 = 3, 4, \ldots, N_1 - 1$, we obtain

$$w_{1,3}^{n+1} \geq \frac{p_{1,5/2} w_{1,2}^{n+1}}{h_1 \rho_{n,n}^1 + p_{1,5/2} + p_{1,7/2}} > 0, \ldots, w_{1,N_1-1}^{n+1} \geq \frac{p_{1,N_1-3/2} w_{1,N_1-2}^{n+1}}{h_1 \rho_{n,n}^1 + p_{1,N_1-3/2} + p_{1,N_1-1/2}} > 0.$$

Finally, from the last equation in (35), we get

$$w_{1,N_1}^{n+1} \geq \frac{2p_{1,N_1-1/2}}{h_1 \rho_{n,n}^1 + 2p_{1,N_1-1/2} + \alpha_1} w_{1,N_1-1}^{n+1} > 0.$$

Applying the same line of considerations for the problem (22), we prove that $0 < w_{2,i_2}^{n+1} \leq 1$, $i_2 = 0, 1, \ldots, N_2$, $j = 1, 2$, $n = 0, 1, \ldots, M - 1$. □

In the same manner, as for the semidiscrete problem, we establish the uniqueness of the solution of the full discrete inverse problem.

Theorem 4. *Let the conditions of Theorem 3 be fulfilled. Then the solution of the full discrete inverse problem* (17)–(18), (30)–(33) *is unique.*

Proof. We follow the same line of considerations as in Theorem 2. We suppose that each of the systems (30)–(33) has two solutions and consider their differences. Then, subtracting the corresponding systems, we derive that these differences are solutions of homogeneous systems of algebraic equations at each time level. Further, since their coefficient matrices are M-matrices, we conclude that they have only trivial solutions. □

5.3. Implementation

Numerical solving of IP[3] performs by the following steps (Algorithm 1):

Algorithm 1 Inverse problem IP[3]

Require: $u_j^0(x_{i_j})$, $\psi_j(t)$, $j = 1,2$.

Ensure: φ_j^{n+1}, u_j^{n+1}, $j = 1,2$, $n = 0,1,\ldots,M$,

$n \leftarrow 0$, $u_{j,i_j}^0 \leftarrow u_j^0(x_{i_j})$, $x_{i_j} \in \overline{\omega}_j$, $j = 1,2$,

while $n < M$ **do**

$u_j^{n+1}(x_j^*) \leftarrow \psi_j^{n+1}$;

Find w_1^{n+1}, solving (32);

Find w_2^{n+1}, solving (33);

Find v_1^{n+1}, solving (30);

Find v_2^{n+1}, solving (31);

Find φ_j^{n+1}, $j = 1,2$ from (23);

Find u_j^{n+1}, $j = 1,2$ from (17) and (18);

$n \leftarrow n + 1$;

end while

6. Extension to 2D Problem

Let $\Omega_j = (a_j, b_j) \times (c, d)$, $\overline{\Omega}_j = \Omega_j \cup \partial\Omega_j$, where $\partial\Omega_j$ is the boundary of the domain $\overline{\Omega}_j$, $j = 1,2$. We introduce the two-dimensional problem

$$
\begin{aligned}
&\frac{\partial^{\delta_1} u_1}{\partial t^{\delta_1}} - \frac{\partial}{\partial x}\left(p_1(x,y)\frac{\partial u_1}{\partial x}\right) - \frac{\partial}{\partial y}\left(q_1(x,y)\frac{\partial u_1}{\partial y}\right) = f_1(x,y,t),\ \ (x,y) \in \Omega_1,\ \ 0 < t \le T,\\
&\frac{\partial^{\delta_2} u_2}{\partial t^{\delta_2}} - \frac{\partial}{\partial x}\left(p_2(x,y)\frac{\partial u_2}{\partial x}\right) - \frac{\partial}{\partial y}\left(q_2(x,y)\frac{\partial u_2}{\partial y}\right) = f_2(x,y,t),\ \ (x,y) \in \Omega_2,\ \ 0 < t \le T,\\
&u_1(a_1,y,t) = \varphi_1(y,t),\ \ u_2(b_2,y,t) = \varphi_2(y,t),\ \ y \in (c,d),\ \ 0 < t \le T,\\
&u_1(x,c,t) = u_{1\mathcal{S}}(x,t),\ \ x \in [a_1,b_1],\ \ u_2(x,c,t) = u_{2\mathcal{S}}(x,t),\ \ x \in [a_2,b_2],\ \ 0 < t \le T,\\
&u_1(x,d,t) = u_{1\mathcal{N}}(x,t),\ x \in [a_1,b_1],\ u_2(x,d,t) = u_{2\mathcal{N}}(x,t),\ x \in [a_2,b_2],\ 0 < t \le T,\\
&p_1(b_1,y)\frac{\partial u_1}{\partial x}(b_1,y,t) + \alpha_1 u_1(b_1,y,t) = \beta_1 u_2(a_2,y,t) + \gamma_1(y,t),\ \ y \in (c,d),\ \ 0 < t \le T,\\
&-p_2(a_2,y)\frac{\partial u_2}{\partial x}(a_2,y,t) + \alpha_2 u_2(a_2,y,t) = \beta_2 u_1(b_1,y,t) + \gamma_2(y,t),\ \ y \in (c,d),\ \ 0 < t \le T,\\
&u_1(x,y,0) = u_1^0(x,y),\ \ (x,y) \in \overline{\Omega}_1, \quad u_2(x,y,0) = u_2^0(x,y),\ \ (x,y) \in \overline{\Omega}_2.
\end{aligned}
\tag{36}
$$

We consider 2D inverse problem, analogical to IP[3], for identifying external boundary conditions $\varphi_j(y,t) = \overline{\varphi}_j(t)\lambda_j(y)$, $j = 1,2$. It is defined by (36) for unknown $\widetilde{\varphi}_j(t)$ and additional point observations

$$
u_j(x_j^*, y_j^*, t) = \psi_j(t),\ \ (x_j^*, y_j^*) \in \Omega_j,\ \ j = 1,2, \tag{37}
$$

Similarly to the 1D case, first we discretize the problem (36) in time, using the L1 formula for approximation of the Caputo derivatives, then we apply the decomposition

$$
u_j^{n+1} = v_j^{n+1} + \overline{\varphi}_j^{n+1} w_j^{n+1},\ \ j = 1,2. \tag{38}
$$

Further, introducing the uniform partition of the spatial domain also $\overline{\omega}_j \times \overline{\omega}_j^y$, where

$$
\overline{\omega}_j^y = \{y_s : y_s = c + sk,\ s = 0,1,\ldots,N_y,\ k = (d-c)/N_y\},
$$

we discretize the decoupled problems in space by a finite difference scheme to obtain

$$
\begin{aligned}
&\rho^1_{n,n} v^{n+1}_{1,i_1,s} - L^x_1 v_{i_1,s} - L^y_1 v_{i_1,s} = f^{n+1}_{1,i_1,s} + G^1_n u^n_{1,i_1,s},\ i_1 = 1,\dots,N_1-1,\ s = 1,\dots,N_y-1,\\
&v^{n+1}_{1,0,s} = 0,\ \ s = 1,2,\dots,N_y-1,\\
&v^{n+1}_{1,i_1,0} = u^{n+1}_{1\mathcal{S},i_1},\ \ v^{n+1}_{1,i_1,N_y} = u^{n+1}_{1\mathcal{N},i_1},\ \ i_1 = 0,1,\dots,N_1,\\
&\left(\rho^1_{n,n} + \frac{2\alpha_1}{h_1}\right) v^{n+1}_{1,N_1,s} + \frac{2}{h_1} p_{1,N_1-1/2,s} v^{n+1}_{1,\bar{x}_{N_1,s}} - L^y_{1,N_1,s}\\
&\qquad = \frac{2\beta_1}{h_1} u^n_{2,0,s} + \frac{2}{h_1}\gamma^{n+1}_{1,s} + f^{n+1}_{1,N_1,s} + G^1_n u^n_{1,N_1,s},\ \ s = 1,2,\dots,N_y-1,\\
&u^0_{1,i_1,s} = u^0_1(x_{1,i_1}),\ \ i_1 = 0,1,\dots,N_1,\ \ s = 0,1,\dots,N_y,
\end{aligned}
\tag{39}
$$

$$
\begin{aligned}
&\rho^2_{n,n} v^{n+1}_{2,i_2,s} - L^x_2 v_{i_2,s} - L^y_2 v_{i_2,s} = f^{n+1}_{2,i_2} + G^2_n u^n_{2,i_2},\ \ i_2 = 1,2,\dots,N_2-1,\\
&\left(\rho^2_{n,n} + \frac{2\alpha_2}{h_2}\right) v^{n+1}_{2,0,s} - \frac{2}{h_2} p_{2,1/2,s} v^{n+1}_{2,x_{0,s}} - L^y_2 v_{0,s}\\
&\qquad = \frac{2\beta_2}{h_2} u^n_{1,N_1,s} + \frac{2}{h_2}\gamma^{n+1}_{2,s} + f^{n+1}_{2,0,s} + G^2_n u^n_{2,0,s},\ \ s = 1,2,\dots,N_y-1,\\
&v^{n+1}_{2,N_2,s} = 0,\ \ s = 1,2,\dots,N_y-1\\
&v^{n+1}_{2,i_2,0} = u^{n+1}_{2\mathcal{S},i_2},\ \ v^{n+1}_{2,i_2,N_{y,2}} = u^{n+1}_{2\mathcal{N},i_2},\ \ i_2 = 0,1,\dots,N_2,\\
&u^0_{2,i_2,s} = u^0_2(x_{2,i_2,s}),\ \ i_2 = 0,1,\dots,N_2,\ \ s = 0,1,\dots,N_y,
\end{aligned}
\tag{40}
$$

$$
\begin{aligned}
&\rho^1_{n,n} w^{n+1}_{1,i_1,s} - L^x_1 w_{i_1,s} - L^y_1 w_{i_1,s} = 0,\ \ i_1 = 1,2,\dots,N_1-1,\ \ s = 1,2,\dots,N_y-1,\\
&w^{n+1}_{1,0,s} = \lambda_{1,s},\ \ s = 1,2,\dots,N_y-1,\\
&w^{n+1}_{1,i_1,0} = w^{n+1}_{1,i_1,N_y} = 0,\ \ i_1 = 0,1,\dots,N_1,\\
&\left(\rho^1_{n,n} + \frac{2\alpha_1}{h_1}\right) v^{n+1}_{1,N_1,s} + \frac{2}{h_1} p_{1,N_1-1/2,s} v^{n+1}_{1,\bar{x}_{N_1,s}} - L^y_1 w_{N_1,s} = 0,\ \ s = 1,2,\dots,N_y-1,
\end{aligned}
\tag{41}
$$

$$
\begin{aligned}
&\rho^2_{n,n} w^{n+1}_{2,i_2,s} - L^x_2 w_{i_2,s_2} - L^y_2 w_{i_2,s_2} = 0,\ \ i_2 = 1,2,\dots,N_2-1,\\
&\left(\rho^2_{n,n} + \frac{2\alpha_2}{h_2}\right) v^{n+1}_{2,0,s_2} - \frac{2}{h_2} p_{2,1/2,s} w^{n+1}_{2,x_{0,s}} - L^y_2 w_{0,s} = 0,\ \ s = 1,2,\dots,N_y-1,\\
&w^{n+1}_{2,N_2,s} = \lambda_{2,s},\ \ s = 1,2,\dots,N_y-1,\\
&w^{n+1}_{2,i_2,0} = w^{n+1}_{2,i_2,N_y} = 0,\ \ i_2 = 0,1,\dots,N_2,
\end{aligned}
\tag{42}
$$

where

$$
\begin{aligned}
&L^x_j v_{i_j,s} = \frac{1}{h_j}\left(p_{j,i_j+1/2,s_j} v^{n+1}_{j,x_{i_j},s} - p_{j,i_j-1/2,s} v^{n+1}_{j,\bar{x}_{i_j,s}}\right),\\
&L^y_j v_{i_j,s} = \frac{1}{k_j}\left(q_{j,i_j,s+1/2} v^{n+1}_{1,y_{i_j},s} - q_{j,i_j,s-1/2} v^{n+1}_{j,\bar{y}_{i_j,s}}\right),\\
&v_{j,x_{i_j,s}} = \frac{v^{n+1}_{j,i_j+1,s} - v^{n+1}_{j,i_j,s}}{h_j},\ \ v_{j,\bar{x}_{i_j,s}} = v_{j,x_{i_j-1,s}},\ \ p_{j,i_j\pm1/2,s} = p_j(x_{j,i_j\pm1/2,s}),\\
&v_{j,y_{i_j,s}} = \frac{v^{n+1}_{j,i_j,s+1} - v^{n+1}_{j,i_j,s}}{k_j},\ \ v_{j,\bar{y}_{i_j,s}} = v_{j,y_{i_j,s-1}},\ \ q_{j,i_j,s\pm1/2} = q_j(x_{j,i_j,s\pm1/2}).
\end{aligned}
$$

Finally, the external boundary conditions are determined from (38) and (37).

$$\overline{\varphi}_j^{n+1} = \frac{\psi_j^{n+1} - v_j^{n+1}(x_j^*, y_j^*)}{w_j^{n+1}(x_j^*, y_j^*)}, \quad j = 1, 2. \tag{43}$$

The correctness of the numerical method (38)–(43) is proved in the same fashion as in Theorem 3.

Proposition 2 (Correctness). *Let* $p_j(x,y) \geq \overline{p}_j(x,y) > 0$, $q_j(x,y) \geq \overline{q}_j(x,y) > 0$, $(x,y) \in \Omega_j$, $j = 1,2$, $\beta_1\beta_2 \leq \alpha_1\alpha_2$, $\alpha_j \geq 0$, $\lambda_{j,s} \geq 0$, $\lambda_{j,s} \not\equiv 0$. *Then* $w^n_{j,i_j,s} \neq 0$, $i_j = 1,2,\ldots,N_j$, $n = 1,2,\ldots,M$, $j = 1,2$,

Proof. It is enough to represent the unknowns $w^n_{j,i_j,s} \neq 0$ in (41), (42) as vectors with length N_jN_y in a system with coefficient matrix of size $N_jN_y \times N_jN_y$. Then, from maximum principle, with similar considerations as in Theorem 3, we derive $0 < w^n_{j,i_j,s} \leq \max\limits_{0\leq s\leq N_y} \lambda_{j,s}$, $i_j = 1,2,\ldots,N_j$, $n = 1,2,\ldots,M$, $j = 1,2$. □

Theorem 5. *Let the conditions of Proposition 2 be fulfilled. Then, the solution of the inverse problem (38)–(43) is unique.*

Proof. The proof follows the same arguments as in Theorem 4. We suppose that each of the problems (39)–(42) has two solutions. Then, their differences are solutions of homogeneous systems with coefficient matrices, which are M-matrices. □

7. Numerical Simulations

In this section, we verify the efficiency of the proposed method. We illustrate the accuracy for the test with weak singular exact solution $u = (u_1, u_2)$ of (1)–(8), and (36), namely with respect to time, there exists a constant C, such that

$$\left|\frac{\partial^k u_j}{\partial t^k}(x,t)\right| \leq C(1 + t^{\delta_j - k}), \quad j = 1,2, \quad k = 0,1,2, \quad \text{for all } (x,t) \in (\overline{\Omega}_1 \cup \overline{\Omega}_2) \times (0,T]. \tag{44}$$

For 1D case, errors of the solution u_j (denoted by $\mathcal{E}_j$), φ_j (denoted by ε_j) and order of convergence in time of φ_j ($\mathcal{CR}^{\varphi}_j$), u_j ($\mathcal{CR}^{\tau}_j$) and spatial convergence rate of u_j ($\mathcal{CR}^{h}_j$) are given by

$$\mathcal{E}_j = \mathcal{E}_j(M, N_j) = \max_{0\leq i_j\leq N_j} \max_{0\leq n\leq M} |u_j(x_{j,i_j}, t_n) - u^n_{j,i_j}|, \quad j = 1,2,$$

$$\varepsilon_1 = \varepsilon_1(M) = \max_{0\leq n\leq M} |u_1(a_1, t_n) - \varphi^n_1|, \quad \varepsilon_2 = \varepsilon_2(M) = \max_{0\leq n\leq M} |u_j(b_2, t_n) - \varphi^n_2|,$$

$$\mathcal{CR}^{\tau}_j = \log_2 \frac{\mathcal{E}_j(M, N_j)}{\mathcal{E}_j(2M, N_j)}, \quad \mathcal{CR}^{h}_j = \log_2 \frac{\mathcal{E}_j(M, N_j)}{\mathcal{E}_j(M, 2N_j)}, \quad \mathcal{CR}^{\varphi}_j = \log_2 \frac{\varepsilon_j(M)}{\varepsilon_j(2M)}.$$

In the case of a 2D problem, we define the errors analogically

$$\mathcal{E}_j = \max_{0\leq i_j\leq N_j} \max_{0\leq s\leq N_y} \max_{0\leq n\leq M} |u_j(x_{j,i_j}, y_s, t_n) - u^n_{j,i_j,s}|, \quad j = 1,2,$$

$$\varepsilon_1 = \max_{0\leq n\leq M} |u_1(a_1, t_n, y_s) - \varphi^n_1|, \quad \varepsilon_2 = \max_{0\leq n\leq M} |u_j(b_2, t_n, y_s) - \varphi^n_2|.$$

In the case, when in $\mathcal{E}_j$ we take the exact solution to be the discrete solution of the corresponding direct problem, we use the notation $\mathcal{E}^h_j$, $j = 1,2$.

We consider the following time grid

$$t_n = T\Big(\frac{n}{M}\Big)^r, \ \ r \geq 1, \ \ n = 0, 1, \ldots, M. \tag{45}$$

If $r = 1$, the mesh is uniform, otherwise the grid nodes are concentrated close to the origin $t = 0$.

Applying similar considerations as in [16], we may deduce that for weak singular solution (44) of (1)–(8) and (36), the order of convergence of the numerical solution, derived by (34) and the corresponding discretization of (36), is

$$\begin{aligned} \mathcal{E} = \max\{\mathcal{E}_1, \mathcal{E}_2\} &\leq O\Big(h_1^2 + h_2^2 + \mu k^2 + M^{-\min\{2-\delta_1, r\delta_1\}} + M^{-\min\{2-\delta_2, r\delta_2\}}\Big) \\ &\leq O\left(h_1^2 + h_2^2 + \mu k^2 + M^{-\min\limits_{j=1,2}\{\min\{2-\delta_j, r\delta_j\}\}}\right), \end{aligned} \tag{46}$$

where $\mu = 0$ for 1D problem and $\mu = 1$ for 2D problem.

In view of (46), in order to obtain optimal accuracy

$$\mathcal{E} \leq O\left(h_1^2 + h_2^2 + \mu k^2 + M^{-\min\limits_{j=1,2}\{2-\delta_j\}}\right), \tag{47}$$

we suggest

$$r = \frac{2-\delta}{\delta}, \ \ \delta = \min\{\delta_1, \delta_2\}. \tag{48}$$

All computations are performed with graded temporal mesh (45), (48).

First, we present computational results for the 1D problem. Let

$$\begin{aligned} &a_1 = 1, \ \ b_1 = 2, \ \ p_1(x) = 2x + 3, \ \ \alpha_1 = 3, \ \ \beta_1 = 2, \\ &a_2 = 3, \ \ b_2 = 5, \ \ p_2(x) = 3x^2 + 1, \ \ \alpha_2 = 1, \ \ \beta_2 = 0.5, \ \ T = 1. \end{aligned} \tag{49}$$

Example 1 (Direct problem)**.** *In this example, we verify the accuracy of the discretization for the direct problem and choice of the temporal mesh.*

For the test example, we determine functions $f_j(x,t)$, $\gamma_j(t)$, $j = 1, 2$, such that

$$u_1(x,t) = E_{\alpha_1}(-t^{\alpha_1})\cos(\pi x/4), \ \ u_2(x,t) = E_{\alpha_2}(-t^{\alpha_2})\cos(\pi x/2),$$

to be the exact solution of the problem (1)–(8), (49). Here, E_{α_j}, $j = 1, 2$ is the Mittag-Leffler function, i.e., $E_\alpha(z) = \sum\limits_{n=0}^{\infty} \frac{z^n}{\Gamma(n\alpha+1)}$.

In order to verify the temporal order of convergence on graded mesh (45), (48), we take $N_1 \gtrsim 0.5M^{(2-\max\{\delta_1,\delta_2\})/2}$, $N_2 = 2N_1$. In Table 1 we give the results for different values of δ_1, δ_2, and M. Obviously the order of convergence in time is $O\big(M^{-(2-\max\{\delta_1,\delta_2\})}\big)$.

Next, we test the order of convergence in space. Let $N_2 = 2N_1$, $M \gtrsim N_2^{2/(2-\delta_1)}$, $\delta_1 = \delta_2 = 0.5$. In Table 2 we list the computational results, which confirm the second-order spatial convergence. Therefore, we may conclude that the convergence of the discretization (34) is the one, given in (47).

Example 2 (Inverse problem: discrete data)**.** *Now, we illustrate the convergence of the numerical solution of the inverse problem. The test problem is* (1)–(8), (49) *with the following right-hand side, boundary, and initial conditions*

$$u_1^0(x)=\cos\frac{\pi x}{4},\ \ u_2^0(x)=\cos\frac{\pi x}{2},\ \ \varphi_1(t)=\frac{\sqrt{2}}{2}E_{\delta_1}(-t^{\alpha_1})+2\begin{cases}\dfrac{t}{T}, & t<\dfrac{T}{2},\\ \dfrac{T-t}{T}, & t>\dfrac{T}{2},\end{cases}$$

$$\varphi_2(t)=0,\ \ f_1(x,t)=2x^2+t^{\delta_1}+t^{2\delta_1}+t,\ \ f_2(x,t)=15E_{\delta_2}(-t^{\alpha_2}),$$

$$\gamma_1=0.5\big(E_{\delta_1}(-t^{\alpha_1})+E_{\delta_2}(-t^{\alpha_1})\big),\ \ \gamma_2=0.$$

Table 1. Errors and temporal convergence rate of the solution (u_1,u_2) of the direct problem (34).

δ_1	δ_2		$M=20$	$M=40$	$M=80$	$M=160$	$M=320$	$M=640$	$M=1280$
0.5	0.5	$\mathcal{E}_1$	5.699×10^{-3}	1.965×10^{-3}	6.157×10^{-4}	2.142×10^{-4}	7.418×10^{-5}	2.600×10^{-5}	9.118×10^{-6}
		$\mathcal{CR}_1^h$	1.536	1.674	1.523	1.530	1.512	1.512	
		$\mathcal{E}_2$	1.844×10^{-2}	6.665×10^{-3}	2.213×10^{-3}	7.720×10^{-4}	2.653×10^{-4}	9.398×10^{-5}	3.286×10^{-5}
		$\mathcal{CR}_2^h$	1.468	1.591	1.519	1.541	1.497	1.516	
0.3	0.6	$\mathcal{E}_\infty$	1.014×10^{-2}	3.113×10^{-3}	1.046×10^{-3}	3.873×10^{-4}	1.462×10^{-4}	5.453×10^{-5}	2.040×10^{-5}
		$\mathcal{CR}_\infty$	1.703	1.573	1.433	1.406	1.423	1.419	
		$\mathcal{E}_2$	3.166×10^{-2}	1.075×10^{-2}	3.496×10^{-3}	1.333×10^{-3}	4.911×10^{-4}	1.859×10^{-4}	6.930×10^{-5}
		$\mathcal{CR}_2^h$	1.559	1.620	1.391	1.441	1.401	1.424	
0.9	0.4	$\mathcal{E}_\infty$	2.672×10^{-2}	9.865×10^{-3}	4.230×10^{-3}	1.988×10^{-3}	8.263×10^{-4}	3.832×10^{-4}	1.684×10^{-4}
		$\mathcal{CR}_\infty$	1.438	1.222	1.089	1.267	1.109	1.186	
		$\mathcal{E}_2$	9.591×10^{-2}	3.127×10^{-2}	1.535×10^{-2}	6.830×10^{-3}	2.907×10^{-3}	1.331×10^{-3}	6.159×10^{-4}
		$\mathcal{CR}_2^h$	1.617	1.026	1.168	1.232	1.127	1.112	

Table 2. Errors and spatial convergence rate of the solution (u_1,u_2) of the direct problem (34).

	$N_1=10$	$N_1=20$	$N_1=40$	$N_1=80$	$N_1=161$	$N_1=320$	$N_1=640$
$\mathcal{E}_1$	1.037×10^{-3}	2.583×10^{-4}	6.445×10^{-5}	1.610×10^{-5}	4.022×10^{-6}	1.005×10^{-6}	2.512×10^{-7}
$\mathcal{CR}_1^h$	2.005	2.003	2.002	2.001	2.000	2.000	
$\mathcal{E}_2$	3.725×10^{-3}	9.320×10^{-4}	2.330×10^{-4}	5.822×10^{-5}	1.455×10^{-5}	3.637×10^{-6}	9.093×10^{-7}
$\mathcal{CR}_2^h$	1.999	2.000	2.000	2.000	2.000	2.000	

The exact solution (u_1,u_2) and the measurements ψ_1, ψ_2 are taken from the discrete direct problem.

On Figures 1 and 2 we plot absolute errors of the identified functions φ_1, φ_1 for different meshes $M=N_1=N_2$, $x_1^*=1.5$, $x_2^*=4$ in the cases $\delta_1=\delta_2=0.5$ and $\delta_1=0.4$, $\delta_2=0.8$. We observe very good accuracy of the restored external boundary condition. As can be expected the bigger error is at point t_1.

In Table 3 we list errors of the solution u and restored functions φ_1, φ_2 for $M=N_1=N_2=160$, $\delta_1=\delta_2=0.5$ and different points of measurements. We observe that the closer the point of the measurement is to the corresponding external boundary, the better the accuracy is. Even for the nonsmooth function φ_1, the restored boundary conditions are very precise. The numerical solution, obtained by the inverse problem is almost the same as the one computed by the discrete direct problem.

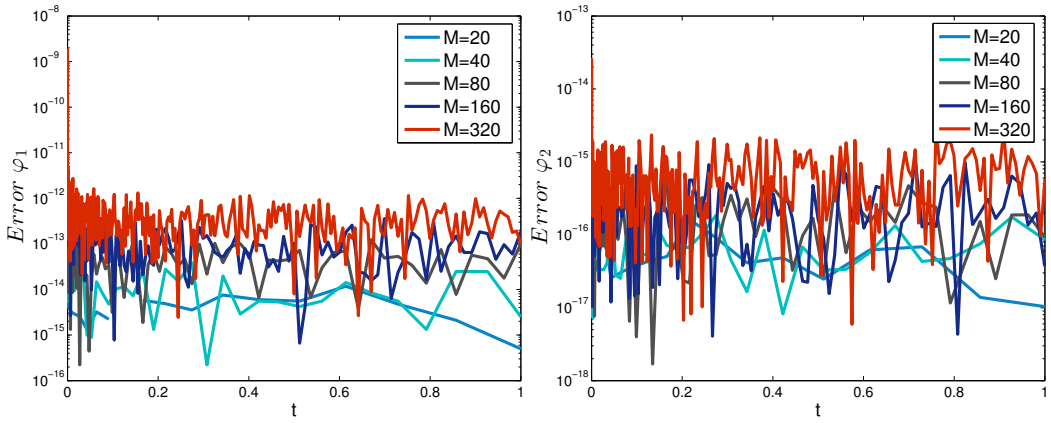

Figure 1. Absolute errors of the recovered φ_1 (**left**) and φ_2 (**right**), $\delta_1 = \delta_2 = 0.5$.

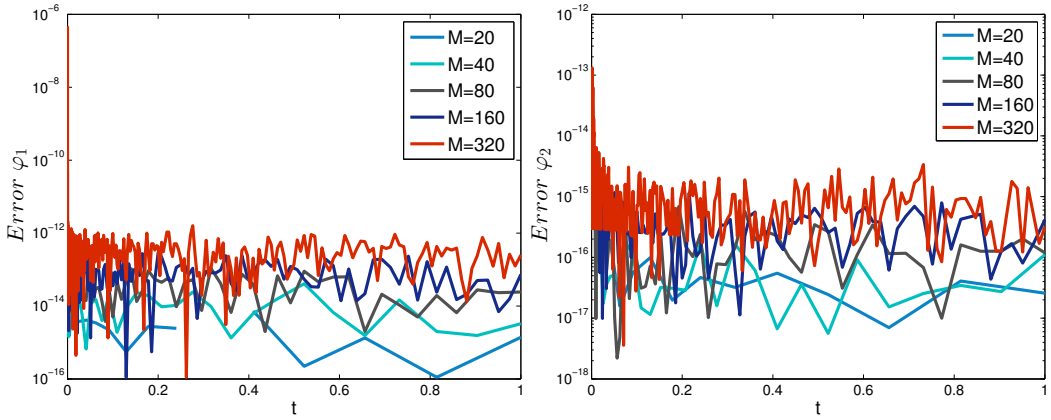

Figure 2. Absolute errors of the recovered φ_1 (**left**) and φ_2 (**right**), $\delta_1 = 0.4$, $\delta_2 = 0.8$.

Table 3. Errors of the solution $(u_1, u_2, \varphi_1, \varphi_2)$ of the inverse problem (19)–(23) for different points of measurement.

Errors	$x_1^* = 1.2$ $x_2^* = 4.8$	$x_1^* = 1.4$ $x_2^* = 4.5$	$x_1^* = 1.5$ $x_2^* = 3.7$	$x_1^* = 1.7$ $x_2^* = 3.5$	$x_1^* = 1.8$ $x_2^* = 3.2$
$\mathcal{E}_1^h$	1.681×10^{-13}	5.189×10^{-13}	1.708×10^{-11}	1.098×10^{-10}	3.389×10^{-10}
$\mathcal{E}_2^h$	2.942×10^{-15}	1.388×10^{-15}	8.707×10^{-15}	5.561×10^{-15}	2.211×10^{-14}
ε_1	2.470×10^{-11}	2.419×10^{-11}	7.631×10^{-12}	8.504×10^{-11}	3.636×10^{-10}
ε_2	1.490×10^{-16}	4.444×10^{-16}	8.707×10^{-15}	5.561×10^{-15}	2.211×10^{-14}

In Figure 3, we depict the numerical solution in the whole time-space computational domain, of the inverse problem (Algorithm 1) for $N_1 = N_2 = M = 40$, $\delta_1 = \delta_2 = 0.5$.

Example 3 (Inverse problem: noisy data). *We consider perturbed input data [3]*

$$\psi_j^{\epsilon}(t^{n^*}) = \psi_j(t^{n^*}) + 2\epsilon_j(\sigma_j(t^{n^*}) - 0.5), \quad j = 1, 2,$$

where ϵ_j^n are noise levels and $\sigma_j(t)$ is a random function, uniformly distributed on the interval $[0, 1]$. The measurements are at $x_1^* = 1.5$, $x_1^* = 4$. In Figure 4, we plot the solution in the whole computational domain of the direct problem and inverse problem with noise at all time levels, i.e., $n^* = n$ for $M = 40$, $N_1 = N_2 = 80$. In Figure 5, we depict the corresponding solution for noisy data at 15 time levels, i.e., $n^* = 15$. In order to obtain noisy values at all time levels and to smooth the functions ψ_1^{ϵ}, $j = 1, 2$, we apply linear and cubic spline interpolation. The resulting graphics are given on the left and right plots.

We observe much better results for the solution, obtained by linear interpolation of the noisy data. Computations showed that to obtain more precise results a bigger number of measurements should be taken near the initial time than near the final time.

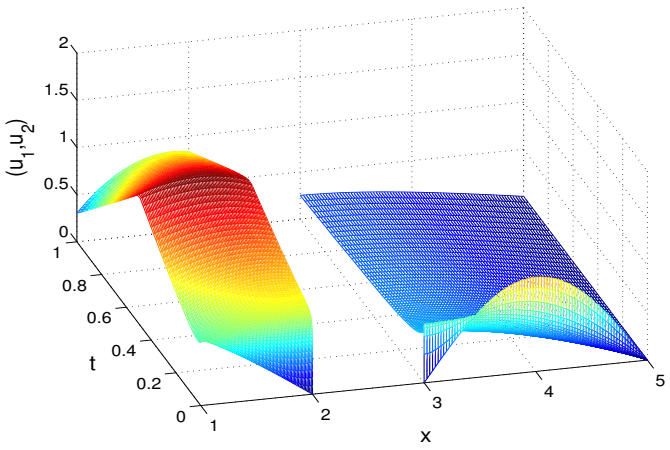

Figure 3. Numerical solution on time-space grid of the inverse problem, $\delta_1 = \delta_2 = 0.5$.

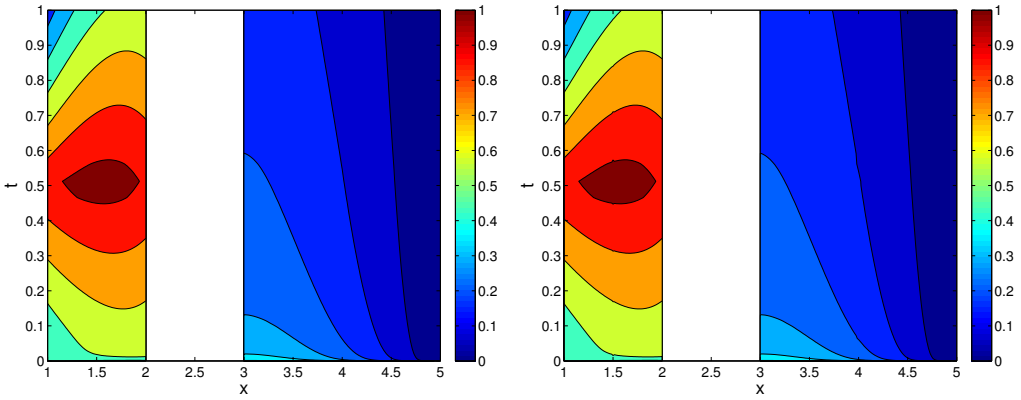

Figure 4. Discrete solution (u_1, u_2) of the direct problem (**left**) and the inverse problem with noisy data at all time levels (**right**), $\delta_1 = \delta_2 = 0.5$.

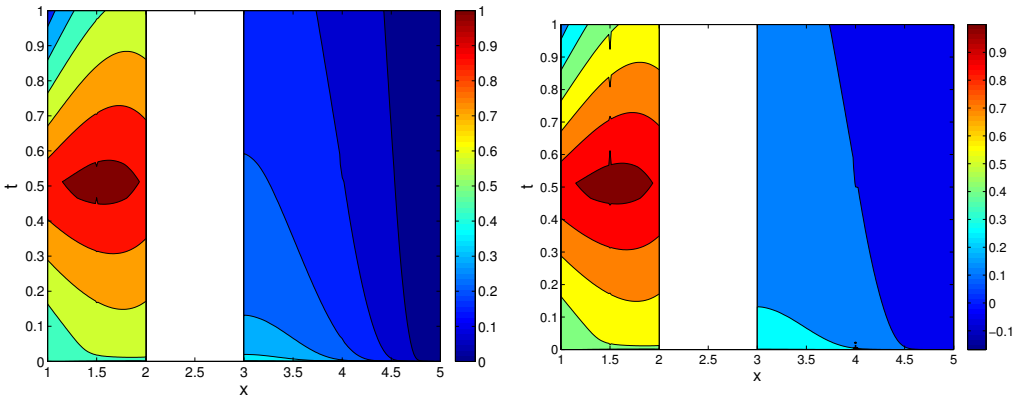

Figure 5. Discrete solution (u_1, u_2) of the inverse problem with measurements at 15 time levels, linear (**left**) and spline (**right**) interpolation for smoothing the functions ψ_1^ϵ and ψ_2^ϵ, $\delta_1 = \delta_2 = 0.5$.

Example 4 (2D inverse problem). *We consider the inverse problem* (36)–(37) *for unknown* φ_j, $j = 1, 2$, *with the following model parameters and functions* $a_1 = 1$, $b_1 = 2$, $a_2 = 3$, $b_2 = 4$, $c = 0$, $d = 1$, $\alpha_1 = 3$, $\alpha_2 = 1$, $\beta_1 = 2$, $\beta_2 = 0.5$, $T = 1$, $N_1 = N_2 = N_y = M = 80$, $p_1(x, y, t) = 3 + 2x + y$, $p_2(x, y, t) = 1 + 3x^2 + 2y$, $q_1(x, y, t) = 1 + x^2 + y^2$, $q_2(x, y, t) = 1 + xy$, $\overline{\varphi}_j(t) = E_{\alpha_j}(-t^{\alpha_j})$, $j = 1, 2$. *To verify the efficiency of the method* (38)–(43), *we use a test*

with an exact solution. Functions γ_j, f_j, λ_j, and Dirichlet boundary conditions are determined such that the exact solution of the problem (36) is

$$u_1(x,y,t) = E_{\alpha_1}(-t^{\alpha_1})(\cos(\pi x/4) + \cos(\pi y/4)),$$
$$u_2(x,y,t) = E_{\alpha_2}(-t^{\alpha_2})(\cos(\pi x/2) + \sin(\pi y/2)).$$

In Table 4 we give errors of the restored functions φ_j and errors (with respect to the exact solution and with respect to the discrete solution of the direct problem) of the solution u_j of the inverse problem, computed by (39)–(43) for $\delta_1 = \delta_2 = 0.5$ and different point of measurements. The test also includes the case when at each time level, we choose random point (x_j^*, y_j^*), $j = 1, 2$ from the set of inner grid nodes, see Figure 6 (left). The values of the measurements are equal to the numerical solution of the direct problem at points (x_j^*, y_j^*, t^{n+1}), $j = 1, 2$, $n = 1, 2, \ldots, M$.

We observe that for measurements far away from the external boundaries the precision of the restored φ_j is a little bit lower, but the error is still very small. Even, when the measurements are at arbitrary points, we attain a very good fitting of the recovered φ_j to the exact one. In Figure 6 (right), we plot the error of the numerical solution of the inverse problem at the final time with measurements shown in Figure 6 (left), compared with the exact solution of the direct problem. The bigger error is attained at the interface boundaries, since the error of the restored external boundary conditions is almost zero. For that reason, for all tests (Table 4), the error $\mathcal{E}_j$ is almost the same. We conclude that the numerical solution of the inverse problem (u_1, u_2) is not so sensitive to the position of the measurements.

Table 4. Errors of $(u_1, u_2, \varphi_1, \varphi_2)$ of the inverse problem (39)–(43) for different points of measurement.

Errors	$x_1^* = 1.5, y_1^* = 0.15$ $x_2^* = 3.5, y_2^* = 0.65$	$x_1^* = 1.65, y_1^* = 0.85$ $x_2^* = 3.25, y_2^* = 0.5$	**random** (x_j^*, y_j^*), $j = 1, 2$, **Figure 6**
$\mathcal{E}_1$	7.587×10^{-4}	7.587×10^{-4}	7.587×10^{-4}
$\mathcal{E}_2$	5.793×10^{-4}	5.793×10^{-4}	5.793×10^{-4}
$\mathcal{E}_1^h$	5.120×10^{-13}	3.036×10^{-12}	5.623×10^{-12}
$\mathcal{E}_2^h$	3.653×10^{-14}	7.505×10^{-14}	3.131×10^{-14}
ε_1	2.999×10^{-13}	1.778×10^{-12}	3.294×10^{-12}
ε_2	1.743×10^{-14}	3.753×10^{-14}	1.465×10^{-14}

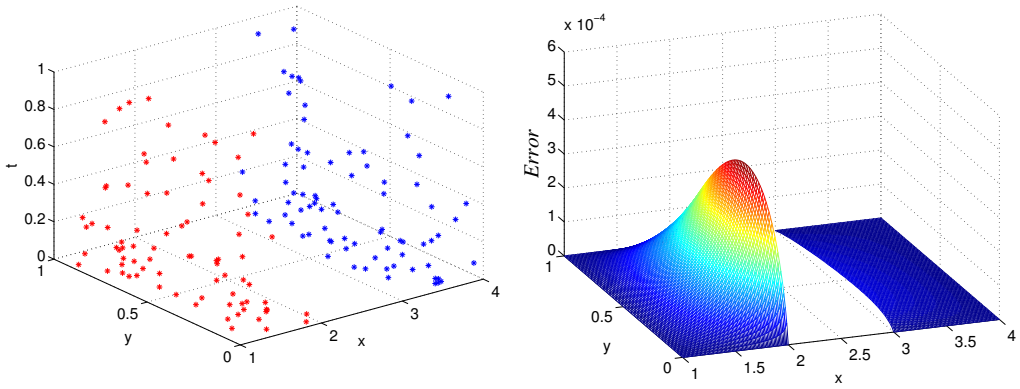

Figure 6. Points of measurements (**left**) and error (**right**) between numerical solution of the inverse problem (u_1, u_2) and exact solution of the direct problem at final time.

8. Conclusions

In this work, we considered 1D and 2D inverse problems for identifying external boundary conditions in time-fractional parabolic problems on disjoint domains. We construct a decomposition method, based on decoupling of the problem at each time level. We

propose an efficient grading of the temporal mesh, such that it handles the weak singularity of the solution in the case of different fractional orders of the equations in each domain. Computational results showed very high accuracy of the restored boundary conditions, even in the case when they are nonsmooth functions of the time. The closer the measurements are to the corresponding external boundary, the more accurate the restored boundary conditions are.

The computed by inverse method solution of the problem is not significantly influenced by the location of the points of the measurements. The solution, obtained by numerically solving the inverse problem is almost the same, as the one computed by the direct problem with the larger error at the interface boundaries, since the error of the recovered external boundary is negligible. The method can be successfully applied in cases where the measurements are not at each time level.

For the point observation, if we have to determine Neumann or Robin external boundary conditions with an unknown right-hand side (source), the present approach can be applied in the same manner. However, if we consider for example final time observation, integral observation, etc., there are no such results in the literature for the present disjoint problems and it requires further investigation. This is out of the frame of the present work, and it will be subject of the future studies. Also, rigorous analysis of the existence and uniqueness of the solution of the present differential inverse problem(s) will be investigated in our forthcoming work.

Author Contributions: Conceptualization, L.G.V.; methodology, M.N.K. and L.G.V.; investigation, M.N.K. and L.G.V.; resources, M.N.K. and L.G.V.; writing—original draft preparation, M.N.K. and L.G.V.; writing—review and editing, M.N.K. and L.G.V.; visualization, M.N.K. All authors have read and agreed to the published version of the manuscript.

Funding: This research was supported by the Bulgarian National Science Fund under Project KP-06-N 62/3 "Numerical methods for inverse problems in evolutionary differential equations with applications to mathematical finance, heat-mass transfer, honeybee population and environmental pollution", 2022.

Data Availability Statement: Not applicable.

Acknowledgments: The authors would like to give special thanks to the anonymous reviewers, whose valuable comments and suggestions have significantly improved the quality of the paper.

Conflicts of Interest: The authors declare no conflict of interest.

References

1. Hasanoglu, A.H.; Romanov, V.G. *Introduction to Inverse Problems for Differential Equations*, 1st ed.; Springer: Cham, Switzerland, 2017; 261p.
2. Lesnic, D. *Inverse Problems with Applications in Science and Engineering*; CRC Press: Abingdon, UK, 2021; p. 349.
3. Samarskii, A.A.; Vabishchevich, P.N. *Numerical Methods for Solving Inverse Problems in Mathematical Physics*; de Gruyter: Berlin, Germany, 2007; p. 438
4. Koleva, M.; Milovanović Jeknić, Z.D.; Vulkov, L. Determination of external boundary conditions of a stationary nonlinear problem on disjoint intervals at point observation. In *Studies in Computational Intelligence*; Springer: Berlin/Heidelberg, Germany, 2022.
5. Zhuo, L.; Lesnic, D.; Meng, S. Reconstruction of the heat transfer coefficient at the interface of a bi-material. *Inverse Probl. Sci. Eng.* **2020**, *28*, 374–401. [CrossRef]
6. Alifanov, O.M. *Inverse Heat Transfer Problems*, 1st ed.; Springer: Berlin/Heidelberg, Germany, 1994; 348p.
7. Amann, H. Maximal regularity of parabolic transmission problems. *J. Evol. Equ.* **2021**, *21*, 3375–3420 . [CrossRef]
8. Caffarelli, L. A monotonicity formula for heat functions in disjoint domains, boundary value problems for partial differential equations and applications. *RMA Res. Notes Appl. Math.* **1993**, *29*, 53–60.
9. Calabro, F.; Zunino, P. Analysis of parabolic problems on partitioned domains withnonlinearconditions at the interface: Application to mass transfer trough semi-permeable membranes. *Math. Model. Methods Appl. Sci.* **2006**, *164*, 479–501. [CrossRef]
10. Datta, A.K. *Biological and Bioenvironmental Heat and Mass Transfer*, 1st ed.; Marcel Dekker: New York, NY, USA, 2002; 424p.
11. Givoli, D. Exact representation on artificial interfaces and applications in mechanics. *Appl. Mech. Rev.* **1999**, *52*, 333–349 [CrossRef]
12. Kinash, N.; Janno, J. An inverse problem for a generalized fractional derivative with an application in reconstruction of time- and space-dependent Sources in fractional diffusion and wave equations. *Mathematics* **2019**, *7*, 1138. [CrossRef]

13. Qatanani, N.; Barham, A.; Heeh, Q. Existence and uniqueness of the solution of the coupled conduction radiation energy transfer on diffuse gray surfaces. *Surv. Math. Its Appl.* **2007**, *2*, 43–58.
14. Caputo, M. Vibrations of infinite viscoelastic layer with a dissipative memory. *J. Acoust. Soc. Am.* **1974**, *56*, 897–904. [CrossRef]
15. Podlubny, I. *Fractional Differential Equations*; Elsevier: Amsterdam, The Netherlands, 1998.
16. Stynes, M.; O'Riordan, E.; Gracia, J.L. Error analysis of a finite difference method on graded meshes for a time-fractional diffusion equation. *J. Numer. Anal.* **2017**, *55*, 1057–1079. [CrossRef]
17. Zhang Y.; Sun Z.; Liao, H. Finite difference methods for the time fractional diffusion equationo non-uniform meshes. *J. Comput. Phys.* **2014**, *265*, 195–210. [CrossRef]
18. Lancia, M. R.; Cefalo, M.; Dell'Acqua, G. Numerical approximation of transmission problems across Koch-type highly conductive layers. *Appl. Math. Comput.* **2012**, *218*, 5453–5473. [CrossRef]
19. El Hamidi, A.; Kirane, M.; Tfayli, A. An Inverse Problem for a Non-Homogeneous Time-Space Fractional Equation. *Mathematics* **2022**, *10*, 2586. [CrossRef]
20. Jovanovic, B.S.; Milovanovic, Z.D. Numerical approximation of a 2D parabolic transmission problem in disjoint domains. *Appl. Math. Comput.* **2014**, *228*, 508–519. [CrossRef]
21. Jovanovic, B.; Koleva, M.; Vulkov, L. Convergence of a FEM and two-grid algorithms for elliptic problems on disjoint domains. *J. Comput. Appl. Math.* **2011**, *236*, 364–374. [CrossRef]
22. Koleva, M. Finite element solution of 1D boundary value linear and nonlinear problems with nonlocal jump conditions. *AIP Conf. Proc.* **2007**, *946*, 163.
23. L'vov, P.E.; Sibatov, R.T.; Yavtushenko, I.O.; Kitsyuk, E.P. Time-Fractional phase field model of electrochemical impedance. *Fractal Fract.* **2021**, *5*, 191. [CrossRef]
24. Milovanovic, Z. Finite difference scheme for a parabolic transmission problem in disjoint domains. *Lect. Notes Comput. Sci.* **2013**, *8236*, 403–410.
25. Prilepko, A.I.; Kamynin, V.L.; Kostin, A.B. Inverse source problem for parabolic equation with the condition of integral observation in time. *J. Inverse -Ill-Posed Probl.* **2018**, *46*, 523–539. [CrossRef]
26. Teresi, L.; Vacca, E. Transmission phenomena across highly conductive interfaces. In *Applied and Industrial Mathematics in Italy II*; Series on Advances in Mathematics for Applied Sciences; World Scientific: Singapore, 2007; pp. 585–596.
27. Vulkov, L. Well posedness and monotone iterative method for nonlinear interface problem on disjoint intervals. *AIP Conf. Proc.* **2007**, *946*, 188.
28. Zhang, Y.; Mazzucato, A.L. Transmission problems for parabolic operators on polygonal domains and applications to the finite element method. *La Mat.* **2022**, *1*, 225–262. [CrossRef]
29. Jovanovic, B.S.; Vulkov, L.G.; Delic, A. Boundary value problems for fractional PDE and their numerical approximation. In *Numerical Analysis and Its Applications*; Dimov, I., Farago, I., Vulkov, L., Eds.; Lecture Notes in Computer Science; Springer: Berlin/Heidelberg, Germany, 2013; Volume 8236, pp. 38–49.
30. Jovanovic, B.S.; Vulkov, L.G.; Delic, A. About some boundary value problems for fractional PDE and their numerical solution. *Proc. Appl. Math. Mech.* **2013**, *13*, 445–446. [CrossRef]
31. Al-Masaeed, R.; Maayah, B.; Abu-Ghurra, S. Adaptive technique for solving 1-D interface problems of fractional order. *Int. J. Appl. Comput. Math* **2022**, *8*, 214. [CrossRef] [PubMed]
32. Vasil'ev, V.I.; Su, L. Numerical method for solving boundary inverse problem for one-dimensional parabolic equation. *Math. Model.* **2017**, *24*, 108–117. [CrossRef]
33. Chen, S.; Jiang, D.; Wang, H. Simultaneous identification of initial value and source strength in a transmission problem for a parabolic equation. *Adv. Comput. Math.* **2022**, *48*, 77. [CrossRef]
34. Kiana, Y.; Oksanenb, L.; Soccorsia, E.; Yamamoto, M. Global uniqueness in an inverse problem for time fractional diffusion equations. *J. Differ. Equ.* **2018**, *264*, 1146–1170. [CrossRef]
35. Ashurov, R.; Fayziev, Y. On the nonlocal problems in time for time-fractional subdiffusion equations. *Fractal Fract.* **2022**, *6*, 41. [CrossRef]
36. Ozbilge, E.; Kanca, F.; Özbilge, E. Inverse problem for a time fractional parabolic equation with nonlocal boundary conditions. *Mathematics* **2022**, *10*, 1479 [CrossRef]
37. Klibas, A.A.; Srivastava H.M.; Trujillo, J.J. *Theory and Applications of Fractional Differential Equations*; Elsevier: Amsterdam, The Netherlands, 2006; p. 540.
38. Hadamard, J. *Lectures on Cauchy's Problem in Linear Partial Differential Equations*; Yale University Press: New Haven, CT, USA, 1923.
39. Evans, L.C. *Partial Differential Equations*, 2nd ed.; American Mathematical Society: Prividence, RI, USA, 2010; Volume 19.
40. Varga, R.S. *Matrix Iterative Analysis*, 2nd ed.; Springer: Berlin/Heidelberg, Germany, 2000; p. 358.